Composites Part B 172 (2019) 143–151

Contents lists available at ScienceDirect

Composites Part B

journal homepage: www.elsevier.com/locate/compositesb

Shear assisted two phase solvent extraction for high dispersion, filler wetting and fracture resistance in quasi-isotropic epoxy nano-composites

Muhammad A.S. Anwer, Yannan Zhou, Hani E. Naguib *

Department of Mechanical and Industrial Engineering, University of Toronto, 5 King's College Street, Toronto, Ontario, Canada

ARTICLE INFO

Keywords:
Particle-reinforcement
Surface treatments
Fracture toughness
Fibre/matrix bond

ABSTRACT

In this work, a novel, simple and scalable methodology, based on in-situ shear assisted solvent exchange in two phases, is used to disperse functionalized carbon nanofibres (CNF) within epoxy. Critical stress intensity factor, K_{IC}, of composites prepared using this method was more than 2.2 times higher than that of neat epoxy at just 0.5-1 wt% filler content. This ranks amongst some of the highest increases observed for such class of nano-composite systems. In comparison to conventional surfactant assisted processing, results from this method showed significantly higher dispersion, adhesion, and fracture resistance. The high dispersion and matrix-filler interactions is further is also indicated by calorimetric and spectroscopic analysis, and evidenced by an increase in the glass transition temperature by almost 10 °C with respect to control through the addition of 1 wt% CNF. The method presented herein is expected to be applicable to a wide array of quasi-isotropic nanocomposite epoxy systems.

1. Introduction

Polymer nano-composites are a promising solution, as light weight materials, to a never ending quest for saving energy. One of the major components in these composites is the matrix or resin which plays the critical role of stress transfer and increasing resistance to fracture propagation throughout the composite. The latter characteristic is important in certain matrix dependant fracture modes within continuous fibre composites such as interlaminar fracture toughness [1]. Epoxies have been a widely utilized choice of matrix resins in continuous fibre composites, primarily due in part to their extremely high strength of adhesion and capacity for load transfer to the fibre skeleton. However, their brittle character results in low fracture toughness (particularly interlaminar) of their composites. In order to increase the fracture characteristics of the polymer matrix resins, various techniques are employed but some of the most common methods remain forming quasi-isotropic composites of the matrix itself with high aspect ratio nano-fillers [2,3]. This promotes extrinsic reinforcement mechanisms during fracture propagation within the matrix like crack bridging, fibre pullout, crack deflection etc. [4] In order for such mechanisms to operate with full efficiency, the wetting and dispersion of nanofillers within the matrix should be complete. Also, adhesion between the matrix and filler plays a critical role in crack initiation resistance and transmission of load to the fillers.

Hence, in an effort to achieve high matrix-filler adhesion and dispersion, much research has been dedicated and the pursuit of this endeavor continues to be of great interest [5–10]. Some of the most effective nano-composite fabrication techniques involve reduction of the surface tension between the matrix and the nano-filler (increasing adhesion) which promotes wetting and transmission of shear energy, in-turn facilitating better dispersion.

Functionalization generally results in both, reduction of surface tension and promotion of matrix-filler adhesion. Functionalization involves grafting of coupling agents (molecules) onto reactive sites (such as –OH, –COOH, -NH2 etc.) on the surface of the filler to potentially create covalent linkages between the filler and matrix [11]. These linkages are formed by separate entities on the coupling agent molecules which bond with the matrix and the sites on the fillers. A number of species have been utilized as coupling agents, which contain reactive sites for both the polymer and the matrix such as silane based coupling agents [5]. Some of the more recent methods include utilization of mussel inspired chemistry where dopamine or catechin molecules are allowed to polymerize and attach to the surface of organic or inorganic substrates. These surface polymer coatings can then be part of a secondary reaction, such as Michael reaction, to introduce thiol or amino groups for reaction with polymer matrices [12–17]. However, many of

* Corresponding author. Department of Mechanical and Industrial Engineering, Department of Materials Science and Engineering, Institute of Biomaterials and Biomedical Engineering, University of Toronto, 5 King's College Street, Toronto, Ontario, Canada.
E-mail address: naguib@mie.utoronto.ca (H.E. Naguib).

https://doi.org/10.1016/j.compositesb.2019.05.088
Received 15 April 2018; Received in revised form 20 December 2018; Accepted 6 May 2019
Available online 9 May 2019

the functionalization methods separate grafting on filler sites from incorporation of the grafted fillers into the matrix due to incompatibility of the matrix with the carrier solvent used to graft the coupling agent and/or create the reactive sites on the surface of the fillers [18–21]. One possible route to overcome this limitation is to use solvent exchange, which is a class of techniques that involve replacement of one solvent with another of a particle solution in-situ. Conventional solvent exchange procedures for nanocomposites include sol-gel based diffusion mediated solvent transfer and are carried out at a slow rate [22,23]. This limits their scope only to applications requiring small amount of fillers to be exchanged at a time [23–25].

Graphitic materials posses rich potential for functionalizability as a result of the constituting sp2 hybridized planes of carbon atoms [26]. CNTs and Graphenes have had the most intensive research focus for functionalization schemes due to their extremely high surface area, strength, stiffness, electrical and thermal conductivity [5,27,28]. However, their prohibitively high expense limits their scope in many applications. CNFs have emerged as low cost alternatives and consist of stacked-cup carbon nanotubes with high mechanical and morphological characteristics [29]. Numerous studies have shown the incorporation of CNFs in a range of matrices to increase their thermal, mechanical, and electrical properties [30,31]. Recently, Liu et al. prepared composites of epoxy and carbon nanofibres wherein polydopamine (PDA) was coated on the surface of the carbon nanofibres followed by solvent-less mixing of the functionalized carbon nanofibres within epoxy using high shear followed by ultrasonication. Compared with unmodified CNFs, the functionalized CNF epoxy composites show higher mechanical properties and fracture toughness ($K_{IC} = 1.42$ vs. $K_{IC} = 1.61$ MPa $m^{1/2}$). Other studies on covalent funtionalization like silanization [32,33] and amine funtionalization [34] and non-covalent functionalization such as polymer chain wrapping [35,36] also show definite improvement in the dispersion and mechanical characteristics of epoxy-CNF composites as compared with neat epoxy.

Herein is reported a novel and facile method to fabricate covalently functionalized quasi-isotropic epoxy carbon nano-fibre (CNF) nanocomposites with a high level of dispersion and adhesion; a two phase solvent extraction process assisted by high shear. In employing this process, CNFs were first functionalized using acid treatment to introduce –OH containing moeties on the surface. Acetone was directly used as the carrier agent for the silane coupling agent. The functionalized CNF-acid solution was then neutralized with water and repeatedly solvent exchanged with a mixture of acetone and coupling agent through ultrasonication and filtration until the aqueous content dropped to around 1 wt%. This solution was then mixed with epoxy resin and the acetone and remaining water was allowed to vaporize. This permitted the inter-filler spaces to then be concentrated and infiltrated respectively by the epoxy resin, thus comprising the second phase of the solvent exchange process. The morphological, fracture, mechanical and thermal characteristics of epoxy-CNF composites prepared using this method are evaluated and compared with epoxy-CNF composites produced using conventional surfactant assisted processing.

2. Materials and methods

2.1. Materials preparation

Epoxy composites with carbon nanofibres were prepared by two means: 1) Solvent exchange assisted method (S.E.A.) and, 2) Surfactant assisted method (S.A.). In the solvent exchange assisted (S.E.A.) method: I) carbon nanofibers (PR-XT-PS-19, Applied Sciences) were functionalized by stirring with a Teflon bar on a magnetic hot plate kept at around 70 °C for 2 h in an acid bath with the following component ratios 3 [H2SO4]:1 [HNO3] by volume. II) The fillers were then kept in solution and filtered with water excessively until the pH was close to 7. III) Acetone with coupling agent ((3-Glycidyloxypropyl)trimethoxysilane, KBM-403 ShinEtsu) was added to this neutralized aqueous solution of CNFs in the ratio 1:1 with respect to the total solution volume (i.e., 1 part by volume of acetone added per 1 part by volume of the CNF solution being added to). IV) This solution was then sonicated for 5 min at an amplitude of 50% (QSonica). This was to ensure diffusion of acetone to the surface of the carbon nano-fibers against the high polarity of water moeties surrounding the surface of the acid treated fillers. V) This overall solution was filtered to half volume before repeating steps III-V until the final water content in solution was around 1 wt% as per calculation. In this method, the content of the original solvent (water) is reduced in a stepwise manner to half its content in the previous step while maintaining particle dispersion during each step. In the last step, epoxy resin (Fiberglast 2000) was added to the solution and the solution sonicated for 50 min at an amplitude of 50%. Upon completion of this step, the resulting solution was kept for stirring overnight on a hot plate to vaporize acetone and water, leaving behind a solution of epoxy, CNFs and, coupling agent. The coupling agent amount was set to around 0.808 ml per designated wt% of the filler in the final epoxy composite. A schematic of the fabrication methodology is presented in Fig. 1.

For the surfactant assisted preparation (S.A.) of the composites, carbon nanofibers were first sonicated in a solution of acetone and surfactant (Triton X100) for 1 h at an amplitude of 50%. The surfactant amount was kept at 1 ml per 100 ml of acetone and, 2.5 ml of acetone was used per 1 ml of epoxy. Epoxy resin (Fiberglast 2000) was then introduced and the solution was sonicated for another 1 h. Following this, the solution was left to vaporize acetone by stirring overnight on a hot plate. For curing the end products from the two procedures, an amine based hardener was added (Fiberglast 2060) and the resulting mixture stirred and degassed before being cast into the appropriate molds for testing. For DSC and TGA testing, control samples were also prepared using the two methods mentioned above without the addition of carbon nanofibers. Table 1 lists information on the filler content and designations for the composites prepared in this study.

2.2. SENB and tensile testing

ASTM D5045 was used to obtain the fracture characteristics under the single edge notch bend test (SENB) methodology. Liquid epoxy-CNF solutions mixed with the hardener obtained from the solvent exchange assist (S.E.A.) and surfactant assisted (S.A.) methods were degassed, cast into molds and left to cure overnight and further at 60 °C for more than 4 h. The solid epoxy samples obtained were then machined into rectangular samples of approximately 8mm × 16mm × 76.2 mm and post cured at 100 °C for more than 12 h. The samples were chevron notched by a 60° cutter to a depth of 5.08 mm, midway and perpendicular to the side that was 76.2 mm in length. Prior to testing, a sharp razor blade was slid on the chevron notch to create a fresh pre-crack. A schematic of the specimen produced for testing is shown in Fig. 2.

The machined and notched samples were loaded in a three point bending fixture for fracture toughness testing, designed as per the ASTM D5045 standard. A loading rate of 5 mm/min was applied and the load deflection curves from the test were recorded. For calculation of K_{IC}, the maximum load obtained from the load deflection data was utilized. The following expressions were used to calculate the K_{IC} and G_{IC} values based on ASTM D5045:

$$K_{IC} = \left(\frac{P_Q}{BW^{1/2}}\right).f(x) \tag{1}$$

$$f(x) = 6x^{1/2}\frac{[1.99 - x(1-x)(21.5 - 3.93x + 2.7x^2)]}{(1+2x)(1-x)^{3/2}} \tag{2}$$

$$x = a/W \tag{3}$$

$$G_{IC} = U/BW\varphi \tag{4}$$

$$U = U_Q - U_i \tag{5}$$

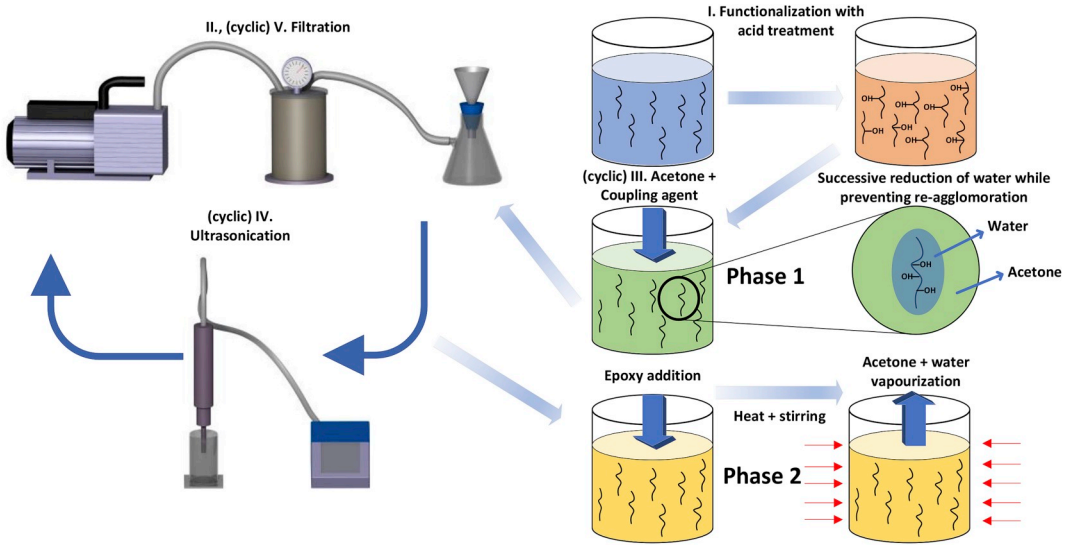

Fig. 1. Schematic of the fabrication methodology. Steps II, III, and IV together form a cyclic process for increasing concentration with the acetone and coupling agent solution while maintaining the state of dispersion through ultrasonication.

Table 1
Designations and preparation methodology for the epoxy carbon nanofiber composites using two phase solvent extraction and surfactant assisted preparation procedures.

Designation	Final filler content in composites	Preparation methodology
0.1 CNF-S.E.A.	0.1 wt% of CNF	Two phase solvent exchange
0.5 CNF-S.E.A.	0.5 wt% of CNF	Two phase solvent exchange
1 CNF-S.E.A.	1 wt% of CNF	Two phase solvent exchange
0.1 CNF-S.A.	0.1 wt% of CNF	Surfactant assist
0.5 CNF-S.A.	0.5 wt% of CNF	Surfactant assist
1 CNF-S.A.	1 wt% of CNF	Surfactant assist
0 CNF-S.E.A.	0 wt% of CNF	Two phase solvent exchange
0 CNF-S.A.	0 wt% of CNF	Surfactant assist

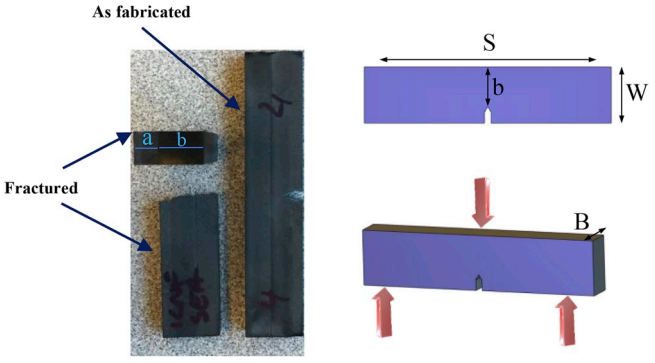

Fig. 2. Schematic showing the samples prepared for SENB testing according to ASTM D5045. B-thickness, b = W (width) - a (crack length), and S-Span.

$$\varphi = \frac{A + 18.64}{dA/dx} \tag{6}$$

$$A = \left[16x^2/(1-x)^2\right]\left[8.9 - 33.717x + 79.616x^2 - 112.952x^3 + 84.815x^4 - 25.672x^5\right] \tag{7}$$

$$dA/dx = \left[16x^2/(1-x)^2\right]\left[-33.717 + 159.232x - 338.856x^2 + 339.26x^3 - 128.36x^4\right] + \left[32x/(1-x)^3\right]\left[8.9 - 33.717x + 79.616x^2 - 112.952x^3 + 84.815x^4 - 25.672x^5\right] \tag{8}$$

Where P_Q is the peak load in the fracture toughness testing, B is the specimen thickness, W is the specimen width, and a is the measured crack length post-fracture testing as shown in the schematic in Fig. 2. U_Q and is the energy obtained by integrating the flexural load-deflection curve of the specimen to fracture initiation and U_i is the corresponding energy from indentation testing as per the ASTM D5045. The data from fracture testing of individual specimens of the epoxy-CNF composites is presented in Supplementary Table S1.

ASTM D638 was used for tensile testing and dog-bone shaped samples were machined out of degassed and cast epoxy CNF solutions prepared using S.E.A. and S.A. methods. The machined samples were post cured at 100 °C for over 4 h prior to testing. The loading rate was set to 5 mm/min as per the ASTM standard.

2.3. MDSC and TGA testing

For MDSC and TGA testing, thin slices weighing approximately 8–25 mg were isolated from the samples prepared using S.E.A (solvent exchange assisted) and S.A. (surfactant assisted) methods respectively with 1 wt% carbon nanofiber concentration. Slices from 0CNF-S.E.A. and 0CNF-S.A. were also prepared for testing (see Table 1). These slices were placed in crimped aluminum pans prior and tested under nitrogen purge in the DSC cell. The samples were first cooled rapidly to 25 °C at a rate of 20 °C/min followed by heating at a rate of 3 °C/min while modulating the temperature ±0.64 °C every 40 s. DSC Q2000 from TA instruments was used for the experimental setup and data recording. For initially determining conditions for thermogravimetric testing, tests were conducted on the samples using a ramp of 20 °C/min to 700 °C to determine degradation onset and evolution (data not presented). Based on the results, isothermal degradation tests were conducted at 900 °C to study mass loss with time.

2.4. Imaging and spectroscopic analysis

High resolution SEM images was taken under field emission micro-

scope (FEI Quanta) on surfaces prepared from notched samples fractured under SENB tests and from cryo-fracturing the samples under liquid nitrogen. The samples were sputter coated with platinum for around 2–3 min prior to testing. TEM imaging was also performed on diamond microtomed sections between 75 and 100 nm thick on a spectrometer enhanced microscope (LEO 912). The sections were placed on copper grids prior to being mounted within the airlock stage. FTIR was done under reflectance on the samples using Bruker Quantachrome. Liquid samples were directly placed on the quartz crystals while solid samples were clamped on the crystal surface to increase signal. XRD and XPS were conducted on the raw CNF powder, neat epoxy, and epoxy with 1 wt% CNF prepared using the S.E.A. and S.A. methodologies. XRD was performed on Philips PW3710 X-ray under ambient conditions using a filtered Cu-Kα radiation of 1.5406 $\mathring{A}$. The generator voltage was set to 40 kV and current to 30 mA. XPS was performed on a thermo scientific K-Alpha machine, and the imaging surfaces for neat epoxy and epoxy with 1 wt% CNFs were prepared prepared using S.E.A. and S.A. assisted methods were fracture surfaces obtained from SENB testing.

3. Results and discussion

3.1. Morphological characteristics

Fig. 3 (a and b) show the SEM images of epoxy composites prepared with 1 wt% CNF using the solvent exchange assisted (S.E.A.) method presented herein (1CNF-S.E.A., Table 1). The sections used for these images were prepared by fracturing the samples pre-cooled under liquid nitrogen. For comparison images produced using the same sectioning procedure on epoxy samples with 1 wt% CNF, using conventional surfactant assisted dispersion (S.A.) are also presented in Fig. 2 (a and b)

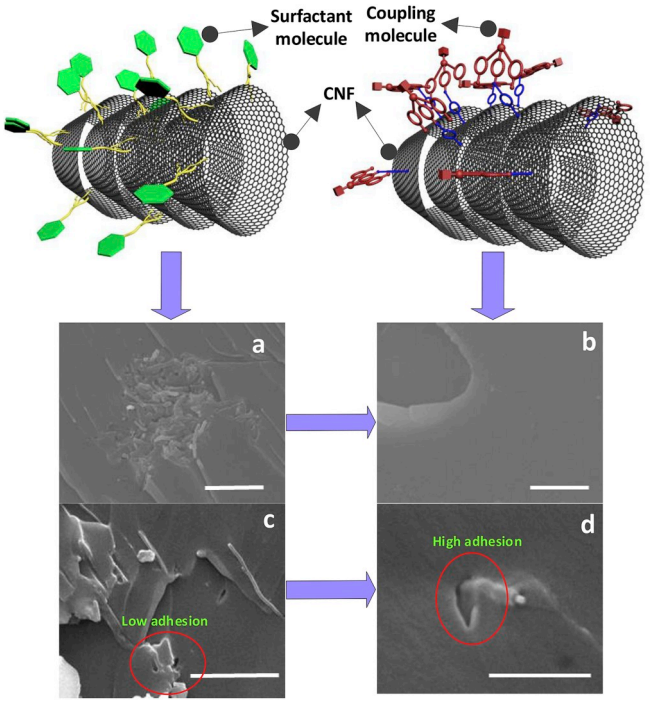

Fig. 3. Internal morphology of a) surfactant assisted (S.A.) and b) solvent exchange assisted (S.E.A.) dispersion of 1 wt% of carbon nano-fiber in epoxy prepared by fracturing samples cooled under liquid nitrogen. Agglomerates and poor fiber-matrix bonding is clearly evident in the former. Fractographs of c) surfactant assisted and d) solvent exchange assisted dispersion of 1 wt% of carbon nano-fiber in epoxy from fracture toughness testing (see methods). Owing to poor adhesion, fiber debonding is significantly greater in the former case. Scale bars (μm): a-5, b-2.5, c-5, and d-1. Schematic of surface modification of carbon nanofibers is shown above (see also Supplementary Fig. S1).

(1CNF-S.A., Table 1). A marked characteristic of samples with surfactant assisted dispersion is the large density of locations with fibers pulled out and de-bonded from the matrix. This is a confirmation of the interface chemical interaction as a result of surfactant coating of the fillers which is solely due to weak dipole moment based interactions. In addition to low adhesion strength, areas of CNF agglomorates with incomplete impregnation of the matrix and the fillers is seen. Since the CNFs were directly mixed into the epoxy, acetone and surfactant solution, the size of the agglomerates depends strongly on adhesive interactions between the filler and the dispersing solution, with stronger adhesion required for promoting greater no-slip condition at the fluid-solid boundary and more effective transfer of dispersive shear forces. In stark contrast, the SEM images of solvent exchange based preparation described herein show much greater and homogenous dispersion and matrix filler wetting. Even in regions where the presence of fiber clusters are evident, the intra-cluster spaces appear to be well infiltrated with epoxy (Supplementary Fig. S1). This is due to epoxy drawn into low pressure inter-filler medium created in wake of vaporization of the acetone and water. Such behaviour is not present in surfactant assisted processing, indicating high adhesion to water and hydrophilicity of CNF after acid treatment which promoted penetration of water into the inter-filler spaces during acid neutralization. The fractographs of the epoxy composites with 1 wt% CNF using both preparation methods are presented in Fig. 3 (c and d). The composites with CNFs using the S.E.A. method show a uniform rough texture across the entire surface. Mechanisms such as crack deflection, crack pinning and fibre pullout are evident on the fracture surface. These features are also present on the fractographs of surfactant assist processed CNF composites however, a marked difference is the significantly lower adhesion of the fibers with the matrix (see Supplementary Fig. S1). Owing to its brittle characteristic in its base state, neat epoxy displays a typical mirror like fracture pattern with few river marks.

The morphological characteristics observed in the SEM images also correlated with internal images obtained using TEM on the epoxy CNF composites slices, as presented in Fig. 4. For the S.A. processed composites, the agglomorates and fiber matrix debonding are clearly visible. In contrast, the dispersion and adhesion in S.E.A. processed composites

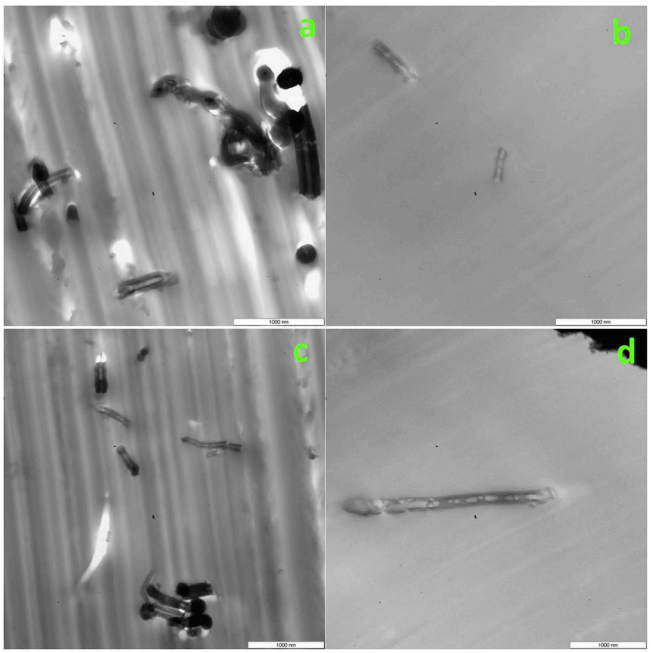

Fig. 4. Transmission electron microscopy (TEM) images of epoxy with 1 wt% CNF composites prepared using S.A. (a and c) and S.E.A (b and d) methodologies. The difference in adheison and dispersion between the two preparation methologies can be clearly seen.

was significantly higher as seen from the much lower visible agglomorate density and CNF debonding. An important characteristic to note is that the CNF length in general is reduced in the S.E.A. processed composites as compared with S.A. processing. This is conformative of the increase in matrix filler adhesion as seen from the SEM images, which results in greater transmission of shear energy and fiber breakdown during S.E.A. composite processing.

3.2. Fracture and mechanical characteristics

Fig. 5 (a, b, and c) show the load deflection curves, trends is K_{IC} and G_{IC} obtained from the fracture toughness testing of the composites of epoxy prepared using the S.E.A. and S.A. methodologies. Table 2 summarizes the results obtained from fracture and mechanical testing. As can be seen, the peak load before catastrophic propagation of failure is much higher in composites with just 0.5-1 wt% of CNF in matrix prepared using S.E.A. method. The net increase over neat epoxy in crack initiation stress intensity factor K_{IC}, is close to 122% with 0.5-1 wt% CNF content. Presented in Fig. 4d is the reported increases in K_{IC} obtained for nanocomposites fabricated with CNTs, Graphenes and Nanoclay reinforcements. In comparison, the increase in K_{IC} over neat epoxy reported herein is amongst the highest for such class of composites. K_{IC} from S.A. preparation is also shown in Fig. 4, which, for 1 wt% CNF concentration, is close to 50% lower than K_{IC} using the S.E.A. method. For the latter, a threshold in increase in K_{IC} is achieved between 0.5 and 1 wt%. The S.A. processed composites do not show a threshold at the same weight content. This is indicative of the agglomerate/cluster size and density reaching disruptive levels at lower weight content in the solvent exchange (S.E.A.) processed composites. Agglomerates increase the particle size and reduce the overall aspect ratio of the reinforcement, hindering the extent of extrinsic reinforcement which would otherwise be present (Supplementary Fig. S2). The greater matrix filler adhesion in the S.E.A. processed composites transmitted larger shear energy to the fillers during ultra-sonication resulting in smaller filler aspect ratio. At smaller aspect ratios, the threshold size of agglomerate at which reinforcement becomes ineffective reduces. The general breakdown of particle size in S.E.A. processing is in conformance with SEM and TEM imaging. Nevertheless, the high matrix-filler adhesion resulted in significant increases in K_{IC} over surfactant assisted (S.A.) processing.

Fiber pullout is a significant contributor to the overall fracture toughness of the nanocomposite.

However, several parameters in the overall pullout process determine the resultant enhancement of the fracture toughness. In general, the pullout process has two mechanisms: i) fibre de-bonding and ii) fibre fracture. The fibre debonding stage itself can be divided into the actual debonding between the fibre and the matrix followed by fibre pullout. The de-bond stress can be expressed as the following expression from the Oliver and Pharr's theory

$$\sigma(x) = \sigma_d + f(x) \tag{9}$$

Where σ_d is the de-bond stress and $f(x)$ is the stress in the fiber caused by friction on the surface of the fiber during pullout. The de-bond stress is expressed below as:

$$\sigma_d = \left(\frac{4E_f G_{2c}}{r_f}\right)^{1/2} \tag{10}$$

Where E_f is the young's modulus of the fibre, G_{2c} is the mode 2 critical strain energy release rate for interfacial cracking and r_f is the radius of the fibre. As a linear approximation, the stress on the surface of the fiber f(x), due to interfacial friction, can be expressed as:

$$\sigma(x) = \frac{2\pi r_f \tau_f x}{\pi r_f^2} = \frac{2\tau_f x}{r_f} \tag{11}$$

Where the $\tau_f = \mu P$ and μ is the coefficient of friction and P is the average compressive stress. As can be seen from eqns. (9)–(11), the primary contributor towards increase in the fracture toughness is the strength of the interface between the fiber and the matrix (G_{2c} for fiber debonding and τ_f for fiber sliding). For the S.E.A. processed composites, SEM and TEM imaging clearly reveal increased adhesion between the fiber and the matrix as compared to the S.A. processed composites implying greater debonding and pullout stress, hence contributing to the significantly larger fracture toughness as seen.

The tensile stress-strain curves properties of the composites prepared

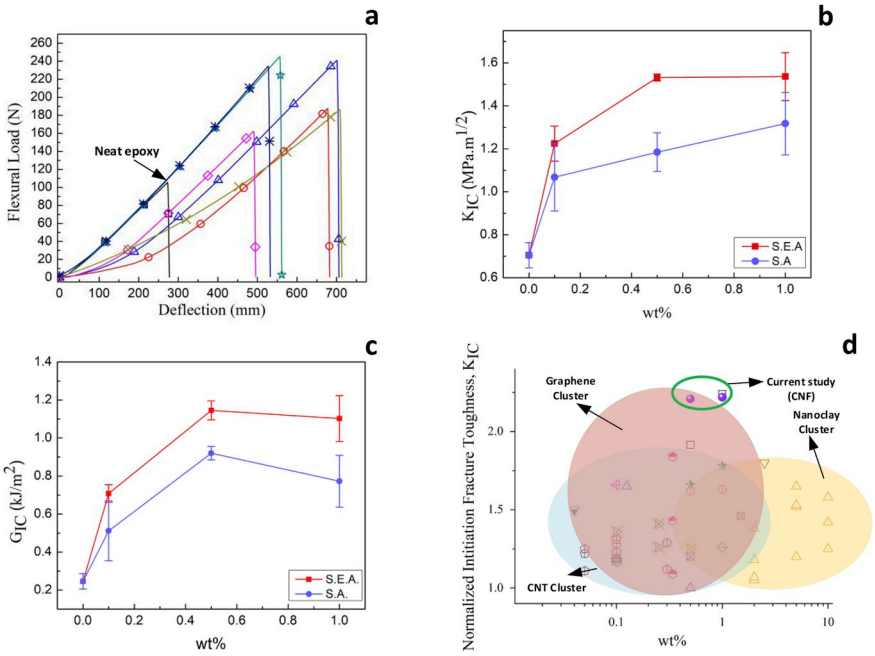

Fig. 5. a) Flexural load and deflection curves of composites of epoxy with CNF prepared using surfactant assited (S.A.) and solvent exchange assisted (S.E.A.) methods (□ neat epoxy, ⋄ 0.1CNF-S.A., × 0.5CNF-S.A., ✳ 1CNF-S.A., ○ 0.1CNF-S.E.A., △ 0.5CNF-S.E.A., ★ 1CNF-S.E.A.). b) Critical stress intensity and c) energy release rate of epoxy CNF composites. d) Comparision of the normalized stress intensity factors from current study with other nanocomposite catagories [40,45–56].

Table 2
Average results from SENB fracture and mechanical testing for the Epoxy-CNF composites.

Composition	K_{IC} (MPa.m$^{1/2}$)	G_{IC} (kJ/m^2)	Normalized Young's Modulus	Tensile Strength (MPa)	Elongation at Break
Neat Epoxy	0.70 ± 0.06	0.246 ± 0.041	1 ± 0.01	59.82 ± 1.63	0.08 ± 0.005
0.1 CNF-S.E.A.	1.22 ± 0.16	0.708 ± 0.046	1.07 ± 0.2	58.2 ± 2.82	0.057 ± 0.0028
0.5 CNF-S.E.A.	1.53 ± 0.02	1.145 ± 0.05	1.09 ± 0.03	51.89 ± 3.72	0.050 ± 0.0057
1 CNF-S.E.A.	1.54 ± 0.11	1.103 ± 0.121	1.04 ± 0.02	60.34 ± 1.5	0.0718 ± 0.0103
0.1 CNF-S.A.	1.06 ± 0.16	0.512 ± 0.158	1.17 ± 0.04	60.34 ± 1.5	0.06 ± 0.005
0.5 CNF-S.A.	1.18 ± 0.09	0.92 ± 0.04	1.19 ± 0.03	61.98 ± 2.76	0.057 ± 0.005
1 CNF-S.A.	1.32 ± 0.15	0.772 ± 0.136	1.13 ± 0.03	68.59 ± 0.59	0.079 ± 0.005

using both methods is shown in Fig. 6 (a, b, c, and d). Compared to S.E.A. processing, the S.A. processed composites show in general a slightly higher Young's modulus. Modulus and strength are bulk mechanical properties which depend strongly on the filler aspect ratio and distribution along with adhesion at the matrix-filler interface [37]. Fracture is a localized process with matrix filler adhesion at the site of stress concentration playing a more predominant role [38]. In composites prepared using S.E.A. processing method, strong matrix filler adhesion helps in supporting localized stresses at the crack tip; increasing the resistance to fracture propagation as already seen [39]. However, the lower damage to aspect ratio in the latter case promotes greater load transmission to the filler throughout the composite bulk, hence resulting in greater stiffness and Young's modulus. The tensile strength for S.E.A. processed composites is also lower compared to surfactant processed composites. As in the case of modulus, the tensile strength is also sensitive to the initial microstructure of the composites with, higher aspect ratio presenting a more significant role than in the case of fracture resistance. Unlike K_{IC}, the tensile strength of the epoxy CNF composites do not show significant enhancements with the addition of CNFs either through the solvent exchange assisted or the surfactant assisted process. CNFs generally consist of stacked cup carbon nanotube structure and are hence composed of multiple layers of graphitic planes which can slide relative to one another. The sliding of graphitic planes is believed to be the result significantly greater enhancement in the fracture toughness behaviour as compared with the tensile strength. This behaviour has also been reported for other layered nano-composites such as GNPs and silicate nanocomposites [40].

3.3. Thermal calorimetric and degradation characteristics

In order to determine the effect of the carbon nanofibers on the glass transition, modulated differential scanning calorimetry (MDSC) was performed. In MDSC, heat energy is applied with sinusoidal intensity to determine the material thermodynamic characteristics which have a single direction of change with temperature change ("irreversible") vs. those characteristics which change in both directions with temperature change ("reversible"). The response to the applied sinusoidal heat flow can be deconvoluted to obtain the reversible and irreversible heat flow components. Glass transition is a reversible change with temperature and is thus obtained as the reversible component of heat flow. The effect of coupling agent on the calorimetric behaviour of epoxy is presented in Fig. 7a. For this, control samples at 0 wt% CNF were also prepared by performing the solvent exchange method for 1 wt% CNF, without adding the nanofibers (0CNF-S.E.A., Table 1). The addition of coupling agent alone reduces the glass transition temperature of neat epoxy by nearly 10 °C. This is a result of plasticization due to the incorporation of the silane coupling agent, into the epoxy network. Literature on the effect of coupling agent alone on epoxy, without the addition of fillers is scant. Two possible mechanisms of epoxy modification by coupling agent are: 1) reaction of oxirane group on the coupling agent with the hardener and 2) pendant incorporation of the coupling agent into the epoxy molecule. Composites with carbon nanofiber at 1 wt% concentration results in a slight increase in the glass transition temperature over neat epoxy. This indicates a nearly 10 °C increase in Tg over the composite prepared without the CNF and with the coupling agent (0CNF-S.E.A.). The large increase in glass transition is due to restriction in chain mobility at the well bonded epoxy carbon nanofiber interface as

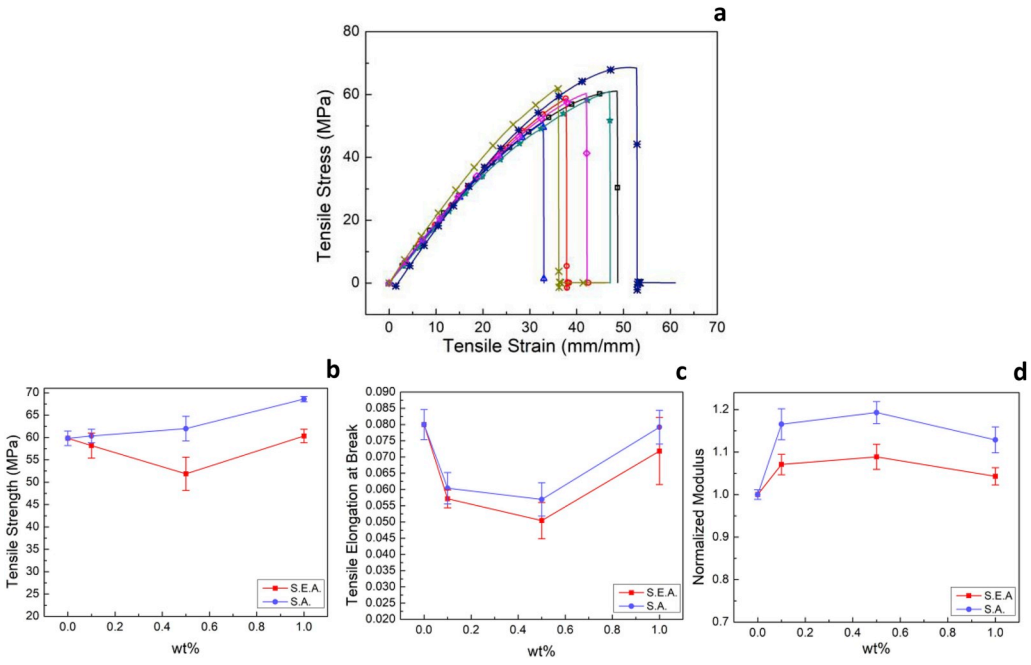

Fig. 6. Tensile stress and strain curves of composites of epoxy with CNF prepared using surfactant assited (S.A.) and solvent exchange assisted (S.E.A.) methods (□ neat epoxy, ⋄ 0.1CNF-S.A., × 0.5CNF-S.A., ✳ 1CNF-S.A., ○ 0.1CNF-S.E.A., △ 0.5CNF-S.E.A., ★ 1CNF-S.E.A.). a) tensile strength, b) tensile elongation at break, and c) normalized modulus of composites with carbon nanofibers in epoxy made using surfactant assist (S.A.) and solvent exchange (S.E.A.) methods. The normalized moudulus was calculated by normalizing the modulus of the nanocomposites w.r.t. the modulus of neat epoxy.

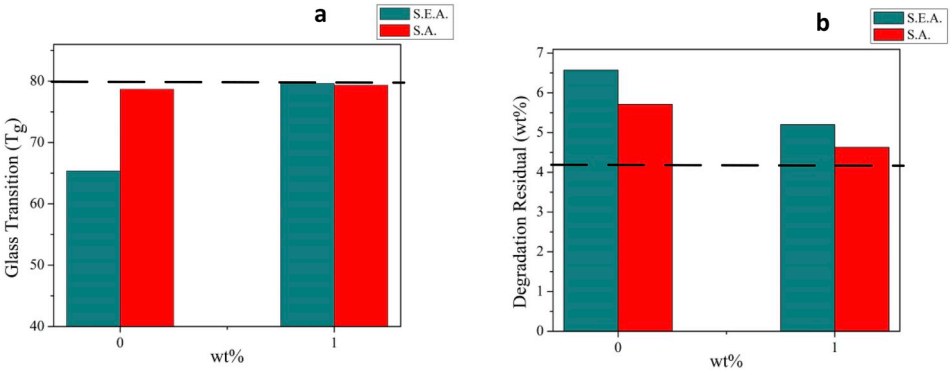

Fig. 7. a) Glass transition and b) isothermal degradation residual of epoxy-CNF composites made using surfactant assist (S.A.) and solvent exchange (S.E.A.) methods. The composites indicated with 0 wt% carbon nanofibers are control samples and have the corresponding amount of coupling agent (0CNF-S.E.A.) or surfactant (0CNF-S.A.) for 1 wt% CNF, without the CNF. The dotted lines represent the y-axis value for neat epoxy. The values presented were extracted from the results of MDSC and isothermal degradation tests respectively (Supplementary Figs. S3 and S4).

evidenced by the SEM images. Control samples of epoxy with Triton corresponding to the amount used to prepared surfactant assisted composites of 1 wt% CNF, without the CNFs (0CNF-S.A.), were also tested and the results shown in Fig. 7a. The glass transition of these samples does not change significantly as compared to neat epoxy, indicating relatively minor effect on temperature induced modification of epoxy network mobility. Thermal degradation behaviour was measured by thin slices of the sample to high temperatures under inert nitrogen atmosphere. Fig. 7b presents the results of the thermogravimetric study. The coupling agent and surfactant alone degrade completely before 500 °C (not shown) and neat epoxy leaves residue of 4.2 wt% by 900 °C. However, samples containing epoxy with 1 wt% CNF prepared using S.E.A. method have a larger residue difference with respect to control, as compared to composites with 1 wt% CNF prepared using S.A. method. This indicates greater interaction between the added CNF and the coupling agent/epoxy mix, in accordance with large adhesion potential as observed from the SEM images and, the expected chemical bonding at the surface of the CNF with the coupling agent.

3.4. Spectral and diffraction analysis

The FTIR spectra of samples prepared with different compositions are presented in Fig. 8. The samples containing epoxy and coupling agent using the S.E.A. process without the CNF, show a peak at frequency of 1543^{-1} which corresponds to one of the peaks of Amide II

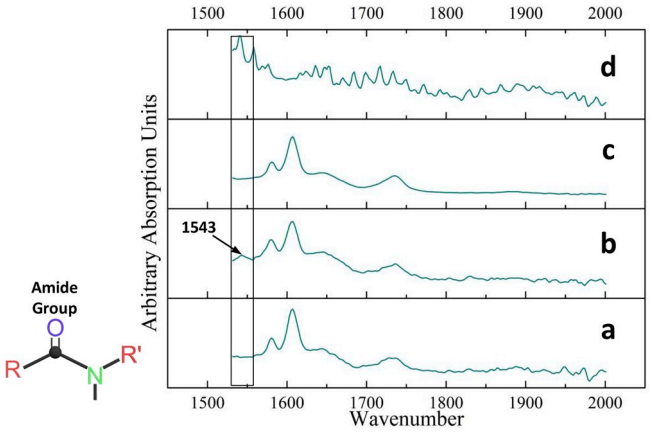

Fig. 8. FTIR absorption spectra a) neat epoxy, b) epoxy with coupling agent prepared using solvent exchange assist for 1 wt% CNF without the addition of CNF (Neat-S.E.A.), c) epoxy with 1 wt% CNF prepared using solvent exchange (1CNF-S.E.A) assist and d) coupling agent. Epoxy with coupling agent (0CNF-S.E.A.) presents an additional peak at 1543^{-1} corresponding to modification Amide 2 bonding not present in either neat epoxy or 1CNF-S.E.A. This is indicative of a chemical modification of the epoxy with the coupling agent which is in part "shielded" with the addition of carbon nanofibers.

characteristic bending mode associated with N-H bonds. This is absent in the composites with neat epoxy, coupling agent and the 1 wt% CNF epoxy produced using the S.E.A. method (1CNF-S.E.A.). Amide II bending mode is conformationally sensitive [41,42]. The presence of such conformational difference is believed to be indicative of alteration of the neat resin network with the coupling agent. With the addition of 1 wt% CNF, the peak at 1543^{-1} disappears which indicates the added coupling agent (silane species) in part is utilized for chemical bonding at the surface of the functionalized carbon nanofibers, which would otherwise have been used to modify neat epoxy.

Fig. 9a) presents the XPS pattern of CNFs, neat epoxy and epoxy with 1 wt% CNF prepared using the S.E.A. and S.A. methodologies. CNF presents two broad peaks centered around 2θ, 26° and 44.8° representing the (002) and (100) planes respectively for graphite [43]. Neat epoxy and 1 CNF S.A. display a broad amorphous peak around 2θ, 17.26° and 16.98° respectively. However, 1 CNF S.E.A. composites show a diffraction peak around 18.32°. The upward shifting of the peak of 1 CNF S.A., as compared to neat epoxy & 1 CNF S.A., is indicative of greater interfacial interaction between the CNFs and epoxy through the S.E.A. process as compared with the S.A. process [44]. Fig. 9b) and c), d) and e) present the XPS spectra of CNFs, neat epoxy, 1CNF S.A., and 1 CNF S.E.A. The atomic% as calculated from XPS are summarized in Table 3. The CNFs display significant peak at C1s followed by O1s with minimal Si2p and N1s peaks. As can be seen, the addition of CNFs to epoxy either through the S.A. or S.E.A. process results in definite increase in the C1s content of the 1 CNF S.A. and 1 CNF S.E.A. composites over neat epoxy.

4. Conclusions

Solvent exchange has been in use extensively as a stand-alone and/or supplementary method to maintain high dispersion of filler particles in nanocomposites while transferring to more suitable solvents for further processing. However, it is usually based on diffusion which limits its wide-scale applicability. This study proposes a novel and facile method to carry out solvent exchange on a nanoparticle suspension in two phases assisted by ultrasonication. Shearing ensures rapid mixing of the solvents at the filler interfaces while maintaining the dispersion of the nanoparticles. Results from this method indicate, at 1 wt% CNF content in the composite, a significant improvement in the crack initiation fracture toughness as compared with neat epoxy. In addition, the dispersion and adhesion between carbon nanofibers and epoxy is significantly improved in comparision with conventional surfactant assisted dispersion as seen from SEM and TEM investigations.

The processing parameters such as solvent mix ratio, amount and ultrasonication shearing conditions can be readily adapted to suit the requirement of the final matrix-filler dispersion state. While this study was conducted with carbon nanofibers, the technique presented can be extended to a range of composite materials systems where the most suitable solvents for each component are different. Engineering high end

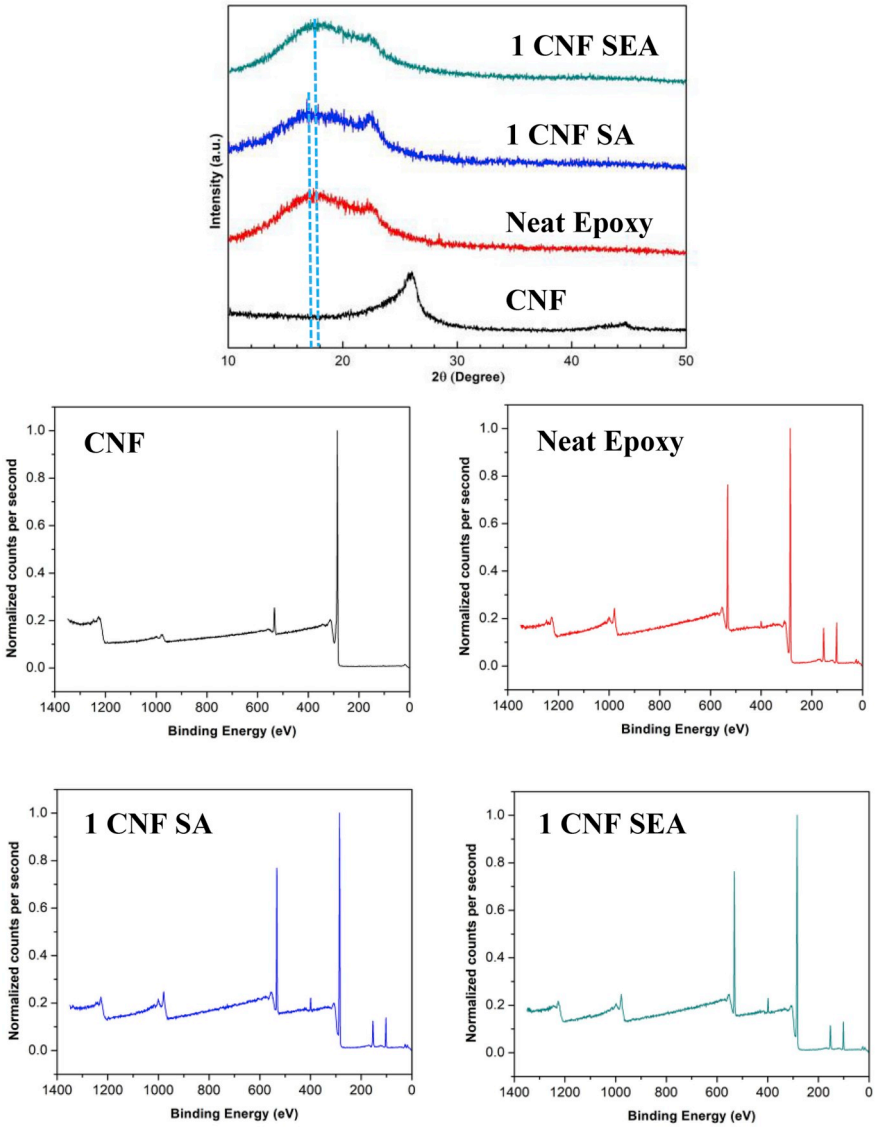

Fig. 9. a) XRD patterns of CNFs neat epoxy, 1 CNF S.A. and 1 CNF S.E.A. composites. Dotted blue lines represents angular shift in peak intensity of 1 CNF SEA as compared with neat epoxy and 1 CNF SA. XPS peaks of b) neat CNF, c) neat epoxy, d) 1 CNF SA and e) 1 CNF SEA. Atomic wt% of the different elements from XPS are presented in Table 3. (For interpretation of the references to colour in this figure legend, the reader is referred to the Web version of this article.)

Table 3
Atomic% of different elements in CNFs, neat epoxy, 1 CNF S.A., and 1 CNF S.E.A. composites as obtained from XPS.

Composition	Si2p	C1s	N1s	O1s
CNF	0.29	93.93	0.22	5.57
Neat epoxy	11.02	68.02	1.77	19.19
1 CNF S.A.	8.51	70.08	2.72	18.69
1 CNF S.E.A.	7.75	70.78	3.17	18.3

mechanical properties of nanocomposites usually requires high dispersion and wetting as a pre-requisite. The results of this study could further other developments in advanced functional materials previously restricted due to requirements of increased matrix-filler dispersion and wetting state.

Acknowledgements

The authors of this work would like to gratefully acknowledge the support from Natural Sciences and Engineering Research Council of Canada (NSERC) [funding reference number(s): PGSD2-504550-2017], Canada Foundation for Innovation (CFI), and Canada Research Chairs (CRC).

Appendix A. Supplementary data

Supplementary data to this article can be found online at https://doi.org/10.1016/j.compositesb.2019.05.088.

References

[1] Chawla KK. Composite materials: science and engineering. Springer Science & Business Media; 2012.
[2] Sun L, Gibson RF, Gordaninejad F, Suhr J. Energy absorption capability of nanocomposites: a review. Compos Sci Technol 2009;69:2392–409.
[3] Domun N, Hadavinia H, Zhang T, Sainsbury T, Liaghat GH, Vahid S. Improving the fracture toughness and the strength of epoxy using nanomaterials - a review of the current status. Nanoscale 2015;7:10294–329. https://doi.org/10.1039/C5NR01354B.
[4] Wegst UGK, Bai H, Saiz E, Tomsia AP, Ritchie RO. Bioinspired structural materials. Nat Mater 2015;14:23–36.

[5] Ma P-C, Siddiqui NA, Marom G, Kim J-K. Dispersion and functionalization of carbon nanotubes for polymer-based nanocomposites: a review. Compos Part A Appl Sci Manuf 2010;41:1345–67.

[6] Jiang R, Liu H, Liu M, Tian J, Huang Q, Huang H, et al. A facile one-pot Mannich reaction for the construction of fluorescent polymeric nanoparticles with aggregation-induced emission feature and their biological imaging. Mater Sci Eng C 2017;81:416–21.

[7] Huang Q, Liu M, Chen J, Wan Q, Tian J, Huang L, et al. Marrying the mussel inspired chemistry and Kabachnik–Fields reaction for preparation of SiO2 polymer composites and enhancement removal of methylene blue. Appl Surf Sci 2017;422:17–27.

[8] Cao Q, Jiang R, Liu M, Wan Q, Xu D, Tian J, et al. Microwave-assisted multicomponent reactions for rapid synthesis of AIE-active fluorescent polymeric nanoparticles by post-polymerization method. Mater Sci Eng C 2017;80:578–83.

[9] Tian J, Jiang R, Gao P, Xu D, Mao L, Zeng G, et al. Synthesis and cell imaging applications of amphiphilic AIE-active poly (amino acid) s. Mater Sci Eng C 2017;79:563–9.

[10] Zhang X, Wang K, Liu M, Zhang X, Tao L, Chen Y, et al. Polymeric AIE-based nanoprobes for biomedical applications: recent advances and perspectives. Nanoscale 2015;7:11486–508.

[11] Kango S, Kalia S, Celli A, Njuguna J, Habibi Y, Kumar R. Surface modification of inorganic nanoparticles for development of organic–inorganic nanocomposites—a review. Prog Polym Sci 2013;38:1232–61.

[12] Zhang X, Liu M, Zhang Y, Yang B, Ji Y, Feng L, et al. Combining mussel-inspired chemistry and the Michael addition reaction to disperse carbon nanotubes. RSC Adv 2012;2:12153–5.

[13] Huang Q, Zhao J, Liu M, Chen J, Zhu X, Wu T, et al. Preparation of polyethylene polyamine@ tannic acid encapsulated MgAl-layered double hydroxide for the efficient removal of copper (II) ions from aqueous solution. J Taiwan Inst Chem Eng 2018;82:92–101.

[14] Zeng G, Chen T, Huang L, Liu M, Jiang R, Wan Q, et al. Surface modification and drug delivery applications of MoS2 nanosheets with polymers through the combination of mussel inspired chemistry and SET-LRP. J Taiwan Inst Chem Eng 2018;82:205–13.

[15] Huang Q, Liu M, Zhao J, Chen J, Zeng G, Huang H, et al. Facile preparation of polyethylenimine-tannins coated SiO2 hybrid materials for Cu2+ removal. Appl Surf Sci 2018;427:535–44.

[16] Zhao J, Huang Q, Liu M, Dai Y, Chen J, Huang H, et al. Synthesis of functionalized MgAl-layered double hydroxides via modified mussel inspired chemistry and their application in organic dye adsorption. J Colloid Interface Sci 2017;505:168–77.

[17] Huang Q, Liu M, Chen J, Wan Q, Tian J, Huang L, et al. Facile preparation of MoS2 based polymer composites via mussel inspired chemistry and their high efficiency for removal of organic dyes. Appl Surf Sci 2017;419:35–44.

[18] Lin Y, Zhou B, Shiral Fernando KA, Liu P, Allard LF, Sun Y-P. Polymeric carbon nanocomposites from carbon nanotubes functionalized with matrix polymer. Macromolecules 2003;36:7199–204. https://doi.org/10.1021/ma0348876.

[19] Sahoo NG, Rana S, Cho JW, Li L, Chan SH. Polymer nanocomposites based on functionalized carbon nanotubes. Prog Polym Sci 2010;35:837–67. https://doi.org/10.1016/j.progpolymsci.2010.03.002.

[20] Ma PC, Kim JK, Tang BZ. Effects of silane functionalization on the properties of carbon nanotube/epoxy nanocomposites. Compos Sci Technol 2007;67:2965–72. https://doi.org/10.1016/j.compscitech.2007.05.006.

[21] Ma P-C, Mo S-Y, Tang B-Z, Dispersion Kim J-K. Interfacial interaction and re-agglomeration of functionalized carbon nanotubes in epoxy composites. Carbon N Y 2010;48:1824–34.

[22] Capadona JR, Van Den Berg O, Capadona LA, Schroeter M, Rowan SJ, Tyler DJ, et al. A versatile approach for the processing of polymer nanocomposites with self-assembled nanofibre templates. Nat Nanotechnol 2007;2:765–9.

[23] Bryning MB, Milkie DE, Islam MF, Hough LA, Kikkawa JM, Yodh AG. Carbon nanotube aerogels. Adv Mater 2007;19:661–4.

[24] Schwertfeger F, Frank D, Schmidt M. Hydrophobic waterglass based aerogels without solvent exchange or supercritical drying. J Non-Cryst Solids 1998;225:24–9.

[25] Wang Y, Shi Z, Fang J, Xu H, Yin J. Graphene oxide/polybenzimidazole composites fabricated by a solvent-exchange method. Carbon N Y 2011;49:1199–207. https://doi.org/10.1016/j.carbon.2010.11.036.

[26] Nunes-Pereira J, Sharma P, Fernandes LC, Oliveira J, Moreira JA, Sharma RK, et al. Poly(vinylidene fluoride) composites with carbon nanotubes decorated with metal nanoparticles. Compos B Eng 1 June 2018;142:1–8. https://doi.org/10.1016/j.compositesb.2017.12.047.

[27] Ioniță M, Vlăsceanu GM, Watzlawek AA, Voicu SI, Burns JS, Iovu H. Graphene and functionalized graphene: extraordinary prospects for nanobiocomposite materials. Compos B Eng 2017;121:34–57. https://doi.org/10.1016/j.compositesb.2017.03.031.

[28] Gao C, Guo Z, Liu J-H, Huang X-J. The new age of carbon nanotubes: an updated review of functionalized carbon nanotubes in electrochemical sensors. Nanoscale 2012;4:1948–63. https://doi.org/10.1039/C2NR11757F.

[29] Anwer MAS, Naguib HE. Study on the morphological, dynamic mechanical and thermal properties of PLA carbon nanofibre composites. Compos B Eng 2016;91:631–9. https://doi.org/10.1016/j.compositesb.2016.01.039.

[30] Raimondo M, Guadagno L, Vertuccio L, Naddeo C, Barra G, Spinelli G, et al. Electrical conductivity of carbon nanofiber reinforced resins: potentiality of Tunneling Atomic Force Microscopy (TUNA) technique. Compos B Eng 2018;143:148–60. https://doi.org/10.1016/j.compositesb.2018.02.005.

[31] Al-Saleh MH, Sundararaj U. A review of vapor grown carbon nanofiber/polymer conductive composites. Carbon N Y 2009;47:2–22. https://doi.org/10.1016/j.carbon.2008.09.039.

[32] Zhu J, Wei S, Ryu J, Budhathoki M, Liang G, Guo Z. In situ stabilized carbon nanofiber (CNF) reinforced epoxy nanocomposites. J Mater Chem 2010;20:4937–48.

[33] Gantayat S, Rout D, Swain SK. Structural and mechanical properties of functionalized carbon nanofiber/epoxy nanocomposites. Mater Today Proc 2017;4:9060–4. https://doi.org/10.1016/j.matpr.2017.07.259.

[34] Karippal JJ, Narasimha Murthy HN, Rai KS, Krishna M, Sreejith M. Effect of amine functionalization of CNF on electrical, thermal, and mechanical properties of epoxy/CNF composites. Polym Bull 2010;65:849–61. https://doi.org/10.1007/s00289-010-0292-z.

[35] Cha J, Jun GH, Park JK, Kim JC, Ryu HJ, Hong SH. Improvement of modulus, strength and fracture toughness of CNT/Epoxy nanocomposites through the functionalization of carbon nanotubes. Compos B Eng 2017;129:169–79. https://doi.org/10.1016/j.compositesb.2017.07.070.

[36] Liu JQ, Xiao T, Liao K, Wu P. Interfacial design of carbon nanotube polymer composites: a hybrid system of noncovalent and covalent functionalizations. Nanotechnology 2007;18:165701.

[37] Ahmed S, Jones FR. A review of particulate reinforcement theories for polymer composites. J Mater Sci 1990;25:4933–42.

[38] Outwater JO, Murphy MC. Fracture energy of unidirectional laminates. Mod Plast 1970;47:160.

[39] Rizvi R, Anwer A, Fernie G, Dutta T, Naguib H. Multifunctional textured surfaces with enhanced friction and hydrophobic behaviors produced by fiber debonding and pullout. ACS Appl Mater Interfaces 2016;8:29818–26. https://doi.org/10.1021/acsami.6b11497.

[40] Zaman I, Kuan H, Meng Q, Michelmore A, Kawashima N, Pitt T, et al. A facile approach to chemically modified graphene and its polymer nanocomposites. Adv Funct Mater 2012;22:2735–43.

[41] Zhang YP, Lewis RNAH, Hodges RS, McElhaney RN. FTIR spectroscopic studies of the conformation and amide hydrogen exchange of a peptide model of the hydrophobic transmembrane. alpha.-helixes of membrane proteins. Biochemistry 1992;31:11572–8.

[42] Stankovich S, Piner RD, Nguyen ST, Ruoff RS. Synthesis and exfoliation of isocyanate-treated graphene oxide nanoplatelets. Carbon N Y 2006;44:3342–7. https://doi.org/10.1016/j.carbon.2006.06.004.

[43] Zhang Z, Deng X, Sunarso J, Cai R, Chu S, Miao J, et al. Two-step fabrication of Li4Ti5O12-coated carbon nanofibers as a flexible film electrode for high-power lithium-ion batteries. 2017. https://doi.org/10.1002/celc.201700351.

[44] Wang Z, Guang-Lin Z. Microwave absorption properties of carbon nanotubes-epoxy composites in a frequency range of 2-20 GHz. Open J Compos Mater 2013;3:17.

[45] Bortz DR, Heras EG, Martin-Gullon I. Impressive fatigue life and fracture toughness improvements in graphene oxide/epoxy composites. Macromolecules 2011;45:238–45.

[46] Rafiee MA, Rafiee J, Srivastava I, Wang Z, Song H, Yu Z, et al. Fracture and fatigue in graphene nanocomposites. Small 2010;6:179–83.

[47] Park YT, Qian Y, Chan C, Suh T, Nejhad MG, Macosko CW, et al. Epoxy toughening with low graphene loading. Adv Funct Mater 2015;25:575–85.

[48] Hollertz R, Chatterjee S, Gutmann H, Geiger T, Nüesch FA, Chu BTT. Improvement of toughness and electrical properties of epoxy composites with carbon nanotubes prepared by industrially relevant processes. Nanotechnology 2011;22:125702. https://doi.org/10.1088/0957-4484/22/12/125702.

[49] Wan Y-J, Tang L-C, Gong L-X, Yan D, Li Y-B, Wu L-B, et al. Grafting of epoxy chains onto graphene oxide for epoxy composites with improved mechanical and thermal properties. Carbon N Y 2014;69:467–80. https://doi.org/10.1016/j.carbon.2013.12.050.

[50] Gojny FH, Wichmann MHG, Köpke U, Fiedler B, Schulte K. Carbon nanotube-reinforced epoxy-composites: enhanced stiffness and fracture toughness at low nanotube content. Compos Sci Technol 2004;64:2363–71. https://doi.org/10.1016/j.compscitech.2004.04.002.

[51] Gojny FH, Wichmann MHG, Fiedler B, Schulte K. Influence of different carbon nanotubes on the mechanical properties of epoxy matrix composites - a comparative study. Compos Sci Technol 2005;65:2300–13. https://doi.org/10.1016/j.compscitech.2005.04.021.

[52] Lachman N, Daniel Wagner H. Correlation between interfacial molecular structure and mechanics in CNT/epoxy nano-composites. Compos Part A Appl Sci Manuf 2010;41:1093–8. https://doi.org/10.1016/j.compositesa.2009.08.023.

[53] Bortz DR, Merino C, Martin-Gullon I. Carbon nanofibers enhance the fracture toughness and fatigue performance of a structural epoxy system. Compos Sci Technol 2011;71:31–8. https://doi.org/10.1016/j.compscitech.2010.09.015.

[54] Kim BC, Park SW. Fracture toughness of the nano-particle reinforced epoxy composite. Compos Struct 2008;86:69–77.

[55] Qi B, Zhang QX, Bannister M, Mai Y-W. Investigation of the mechanical properties of DGEBA-based epoxy resin with nanoclay additives. Compos Struct 2006;75:514–9.

[56] Wang K, Chen L, Wu J, Toh ML, He C, Yee AF. Epoxy nanocomposites with highly exfoliated Clay: mechanical properties and fracture mechanisms. Macromolecules 2005;38:788–800. https://doi.org/10.1021/ma048465n.